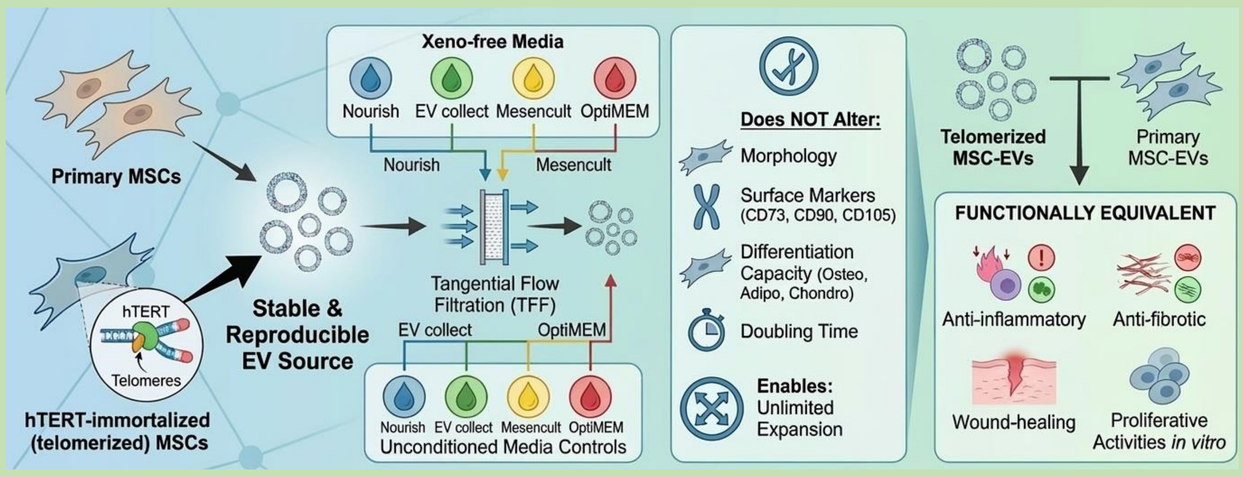
# Immortalization of mesenchymal stromal cells by hTERT does not affect the functional properties of secreted extracellular vesicles

Alessia Brancolini[1], Madhusudhan Reddy Bobbili[2,3,4], Matthias Wieser[1], Johanna Gamauf[1], Marieke Theodora Roefs[1], Matthias Hackl[5], Johannes Grillari [2,3,4], Regina Grillari-Voglauer[1,4]

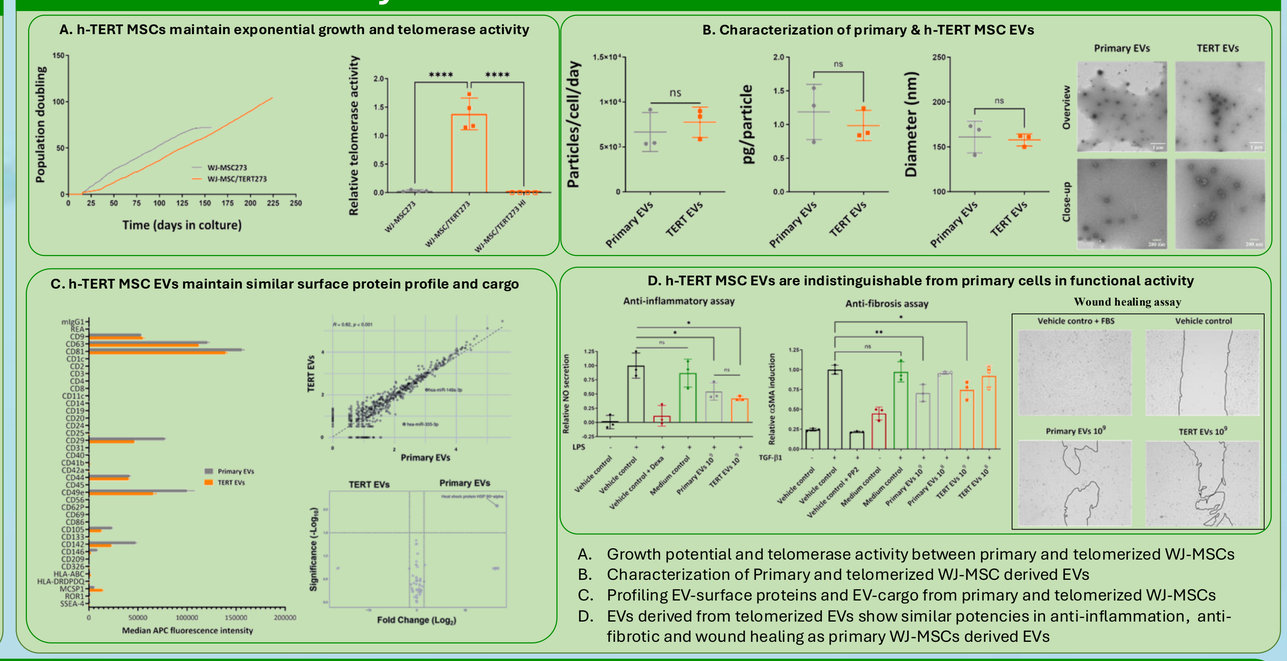
[1] Evercyte GmbH, 1110 Vienna, Austria. [2] Institute of Molecular Biotechnology, Department of Biotechnology and Food Sciences, BOKU University, Vienna, Austria. [3] Ludwig Boltzmann Institute for Traumatology, The Research Center in Cooperation with AUVA, Vienna, Austria. [4]Austrian Cluster for Tissue Regeneration. [5]Tamirna GmbH

## Introduction

Clinical translation of MSC-EVs is hindered by viability from donor heterogeneity, limited primary cell lifespan, and phenotypic drift. This study addresses these challenges by evaluating hTERT-immortalized MSCs for reproducible EV production and systematically assessing the impact of EV collection media



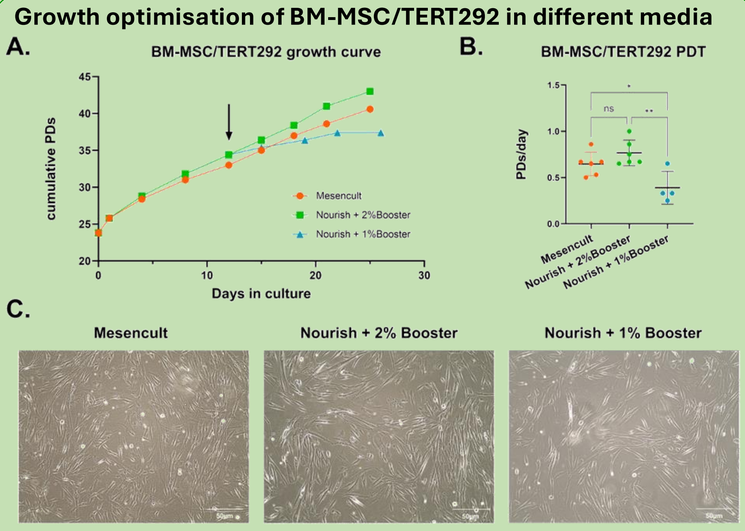

## Primary vs h-TERT immortalized MSCs




A. Growth potential and telomerase activity between primary and telomerized WJ-MSCs
B. Characterization of Primary and telomerized WJ-MSC derived EVs
C. Profiling EV-surface proteins and EV-cargo from primary and telomerized WJ-MSCs
D. EVs derived from telomerized EVs show similar potencies in anti-inflammation, anti-fibrotic and wound healing as primary WJ-MSCs derived EVs

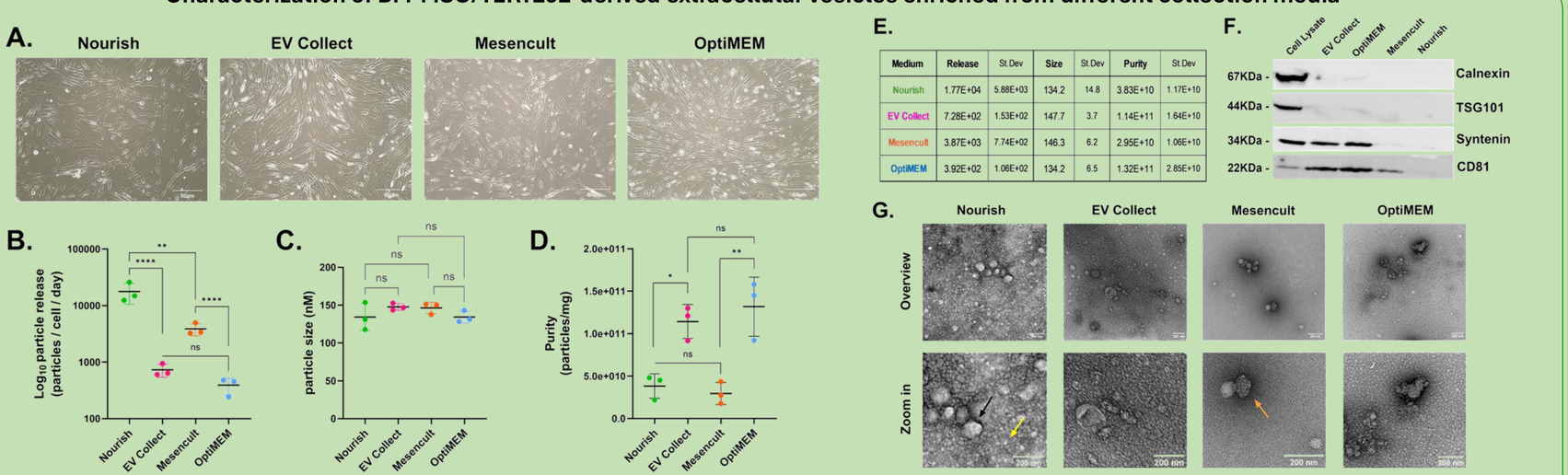
# Role of Growth and Collection Media on hTERT-immortalized MSCs

## Growth optimisation of BM-MSC/TERT292 in different media




**A**. Growth curves of BM-MSC/TERT292 cells in Mesencult (orange dots), Rooster Nourish supplemented with 2% Rooster Booster (green dots) or 1% Rooster Booster (light blue dots). The black arrow indicates the change from 2% to 1% Booster. **B.** Population Doubling Time of BM-MSC/TERT292 cells in Mesencult and Rooster Nourish media supplemented with 2% or 1% Rooster Booster. **C.** Representative microscopy images of BM-MSC/TERT292 cells cultivated in the different media (scale bar: 50µm). Data are represented as mean ± SD; One-way Anova was used, and significance is shown as * $p < 0.05$, ** $p < 0.01$

## Characterization of BM-MSC/TERT292-derived extracellular vesicles enriched from different collection media

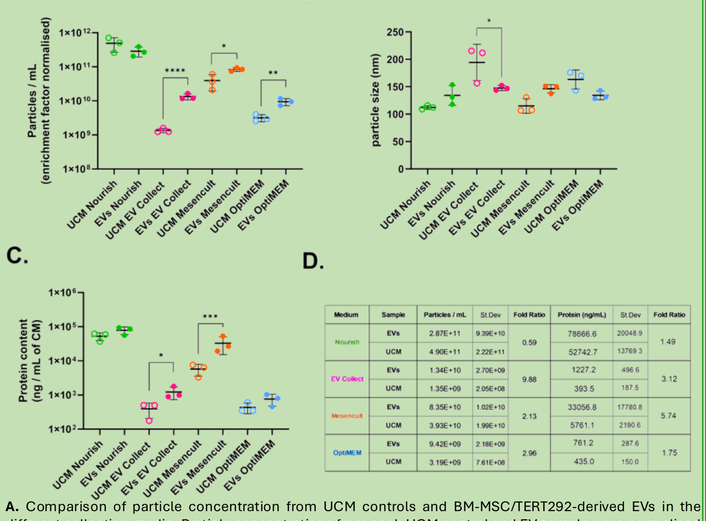



| Medium | Release | St.Dev | Size | St.Dev | Purity | St.Dev |
|---|---|---|---|---|---|---|
| Nourish | 1.77E+04 | 5.88E+03 | 134.2 | 14.8 | 3.83E+10 | 1.17E+10 |
| EV Collect | 7.28E+02 | 1.53E+02 | 147.7 | 3.7 | 1.14E+11 | 1.64E+10 |
| Mesencult | 3.87E+03 | 7.74E+02 | 146.3 | 6.2 | 2.95E+10 | 1.06E+10 |
| OptiMEM | 3.92E+02 | 1.06E+02 | 134.2 | 6.5 | 1.32E+11 | 2.85E+10 |

**A.** Representative microscopy images of BM-MSC/TERT292 cells cultivated in the different media at 48h after last medium exchange as time point of EV harvest (Scale bar: 50µm). **B.** Particle release, **C.** particle size and **D.** purity of BM-MSC/TERT292-derived EVs enriched from different collection media. Data are represented as mean ± SD; For particle release and purity, One-way Anova was performed on $Log_{10}$ transformed data to account for scale difference. For particle size, One-way Anova was performed on untransformed data. Significance is shown as * $p < 0.05$, ** $p < 0.01$, **** p <0.0001 (n=3 independent EV samples/group, each sample from an independent EV batch). **E.** Summary table of mean particle release, particle size and purity for each medium used for EV collection, and relative SD values. **F.** Western blot analysis of common EV surface (CD81) and intraluminal (Syntenin, TSG101) markers, as well as negative EV markers (Calnexin) in BM-MSC/TERT292 cell lysate and secreted EVs in the different collection media. For each EV sample, protein lysate from 1.6E+09 particles was added /lane **G.** Transmission electron microscopy analysis of BM-MSC/TERT292-derived EVs. Black arrow:

# Comparison of the physicochemical properties of EVs and the respective UCM controls

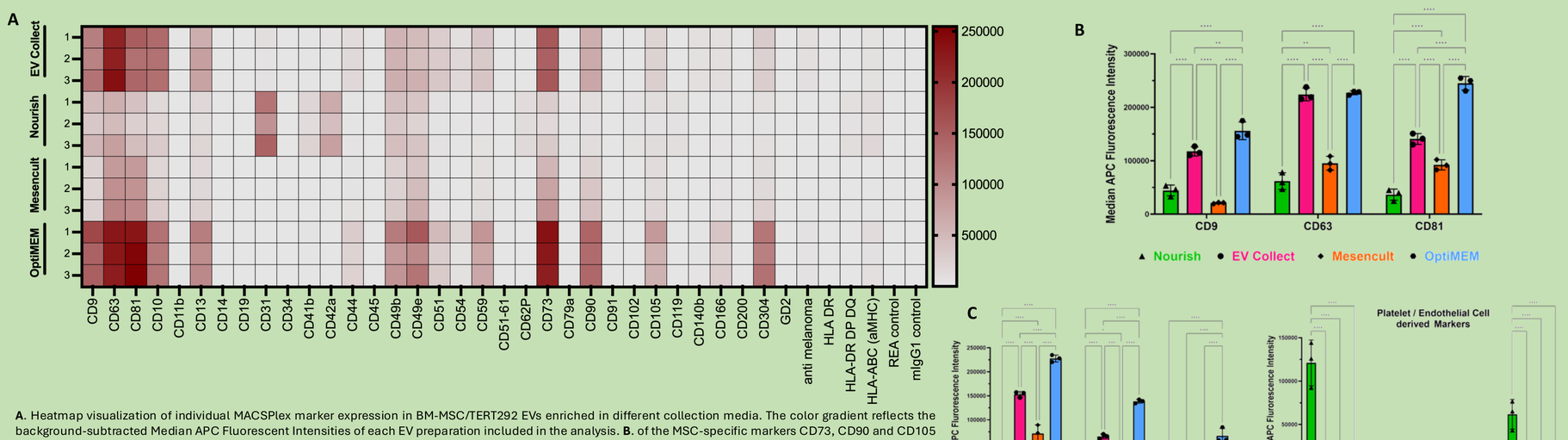
## Physicochemical properties of EVs and UCM controls




| Medium | Sample | Particles / mL | St.Dev | Fold Ratio | Protein (ng/mL) | St.Dev | Fold Ratio |
|---|---|---|---|---|---|---|---|
| Nourish | EVs | 2.87E+11 | 9.39E+10 | 0.59 | 78666.6 | 20048.9 | 1.49 |
| | UCM | 4.90E+11 | 2.22E+11 | | 52742.7 | 13769.3 | |
| EV Collect | EVs | 1.34E+10 | 2.70E+09 | 9.88 | 1227.2 | 496.6 | 3.12 |
| | UCM | 1.35E+09 | 2.05E+08 | | 393.5 | 187.5 | |
| Mesencult | EVs | 8.35E+10 | 1.02E+10 | 2.13 | 33056.8 | 17780.8 | 5.74 |
| | UCM | 3.93E+10 | 1.99E+10 | | 5761.1 | 2190.6 | |
| OptiMEM | EVs | 9.42E+09 | 2.18E+09 | 2.96 | 761.2 | 287.6 | 1.75 |
| | UCM | 3.19E+09 | 7.61E+08 | | 435.0 | 150.0 | |

**A.** Comparison of particle concentration from UCM controls and BM-MSC/TERT292-derived EVs in the different collection media. Particle concentrations from each UCM control and EV sample were normalised on an enrichment factor of 100. **B.** Comparison of particle sizes of UCM controls and BM-MSC/TERT292-derived EVs in the different collection media. **C.** Comparison of protein content / mL of unprocessed CM between UCM controls and BM-MSC/TERT292-derived EVs in the different collection media. **D.** Summary table of mean particle concentration and protein content for UCM controls.

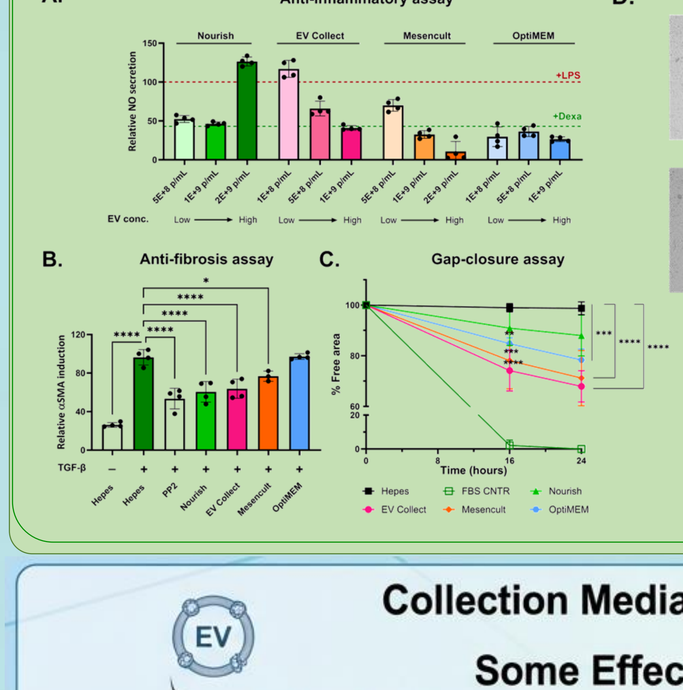
## Surface marker profiling of BM-MSC/TERT292-derived extracellular vesicles enriched from different collection media by MACSPlex analysis




**A.** Heatmap visualization of individual MACSPlex marker expression in BM-MSC/TERT292 EVs enriched in different collection media. The color gradient reflects the background-subtracted Median APC Fluorescent Intensities of each EV preparation included in the analysis. **B.** of the MSC-specific markers CD73, CD90 and CD105 in BM-MSC/TERT292 EVs enriched in different collection media by MACSPlex analysis. **C**. Median APC Fluorescence Intensity of the Platelet and Endothelial cell-derived markers CD31, CD41b and CD42P and CD42a in BM-MSC/TERT292 EVs enriched in different collection media by MACSPlex analysis. For each medium, 3 different EV preparations were analyzed (n=3 independent EV samples/group, each sample from an independent EV batch; the numbers below the heatmap represent each independent EV batch used for the analysis) and data are represented as mean ± SD were applicable. One-way Anova was used, and significance is shown as * $p < 0.05$, ** $p < 0.01$, *** $p < 0.001$, **** $p < 0.0001$

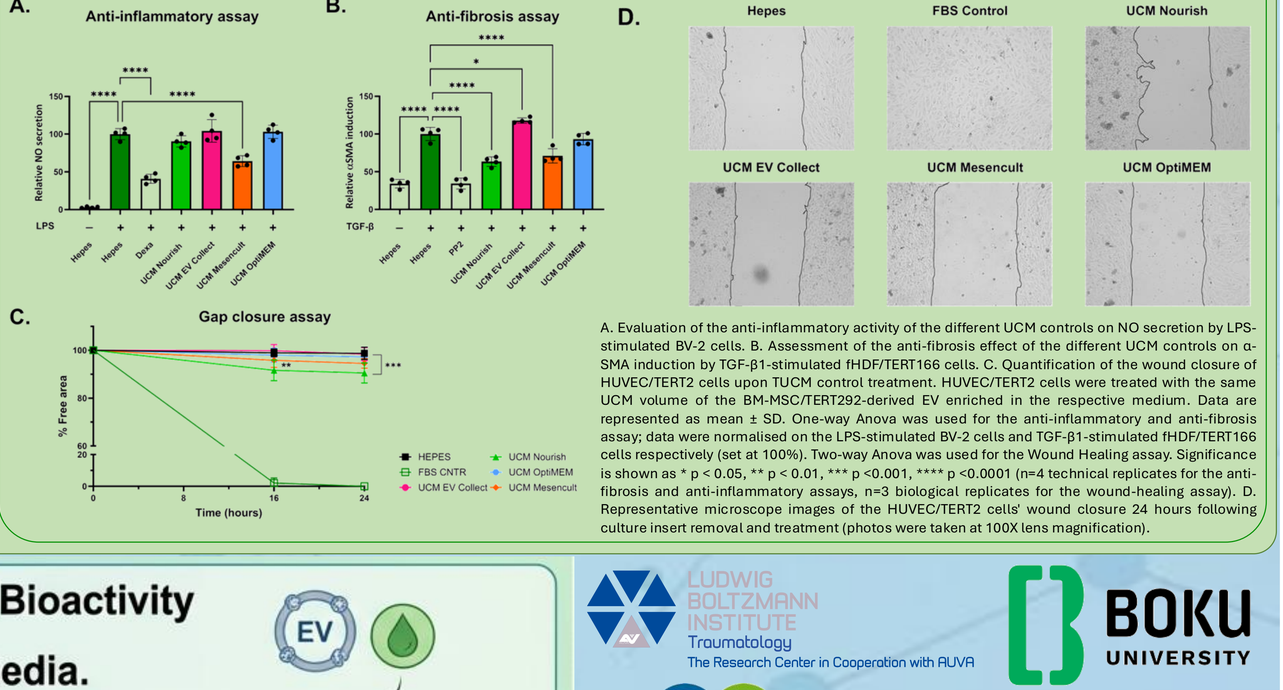
# Comparison of the Biological activity of EVs and the respective UCM controls

## Functional evaluation of BM-MSC/TERT292-derived EVs enriched from different collection media




**A.** Evaluation of the anti-inflammatory activity of BM-MSC/TERT292 EVs enriched from different collection media on nitric oxide (NO) secretion by LPS-stimulated BV-2 cells. **B.** Assessment of the anti-fibrosis effect of BM-MSC/TERT292 EVs enriched from different collection media on α-SMA induction by TGF-β1-stimulated fHDF/TERT166 cells. **C**. Quantification of the wound closure of HUVEC/TERT2 cells upon BM-MSC/TERT292-derived EVs treatment. Data are represented as mean ± SD. One-way Anova was used for the anti-inflammatory and anti-fibrosis assay. Two-way Anova was used for the Wound Healing assay. Significance is shown as * $p < 0.05$, ** $p < 0.01$, *** p <0.001, **** p <0.0001 (n=4 technical replicates for the anti-fibrosis and anti-inflammatory assays, n=3 biological replicates for the wound-healing assay). **D.** Representative microscope images of the HUVEC/TERT2 cells' wound closure 24 hours following culture insert removal and treatment (photos were taken at 100X lens magnification).

## Functional evaluation of different un-conditioned media controls




A. Evaluation of the anti-inflammatory activity of the different UCM controls on NO secretion by LPS-stimulated BV-2 cells. B. Assessment of the anti-fibrosis effect of the different UCM controls on α-SMA induction by TGF-β1-stimulated fHDF/TERT166 cells. C. Quantification of the wound closure of HUVEC/TERT2 cells upon TUCM control treatment. HUVEC/TERT2 cells were treated with the same UCM volume of the BM-MSC/TERT292-derived EV enriched in the respective medium. Data are represented as mean ± SD. One-way Anova was used for the anti-inflammatory and anti-fibrosis assay; data were normalised on the LPS-stimulated BV-2 cells and TGF-β1-stimulated fHDF/TERT166 cells respectively (set at 100%). Two-way Anova was used for the Wound Healing assay. Significance is shown as * $p < 0.05$, ** $p < 0.01$, *** p <0.001, **** p <0.0001 (n=4 technical replicates for the anti-fibrosis and anti-inflammatory assays, n=3 biological replicates for the wound-healing assay). D. Representative microscope images of the HUVEC/TERT2 cells' wound closure 24 hours following culture insert removal and treatment (photos were taken at 100X lens magnification).

## Collection Media Significantly Affects EV Yield & Bioactivity

## Some Effects Overlap with Unconditioned Media.

## MUST Distinguish EV-Specific Effects from Medium-Derived Components

Email: Regina.grillari@evercyte.com Johannes.grillari@lbg.ac.at Alessia.brancolini@evercyte.com Madhusudhan.Bobbili@boku.ac.at

LUDWIG BOLTZMANN INSTITUTE Traumatology The Research Center in Cooperation with AUVA
BOKU UNIVERSITY
EVERCYTE
EU Horizon Europe MSCA Doctoral Network (grant number 101072766)